Fixture Planning With Friction

Soo Hong Lee

M. R. Cutkosky
Center for Design Research,
Mechanical Engineering Dept.,
Stanford University,
Stanford, CA 94305

A fixture planning module is being developed as part of a computational system for concurrent product and process design. The module employs symbolic and numerical analyses at different levels of detail, from fast geometric checks to more time consuming force and friction analyses, depending on the completeness of the machining plan. In this paper we focus on the approaches used for analyzing fixture kinematics and clamping forces, including the analysis of friction. Since many fixture arrangements rely on friction to hold a part, the ability to reason about friction is an important component of fixture planning. Limit surfaces in force/moment space are introduced as a convenient formalism to check whether parts will slip and to help in specifying clamping forces.

1 Introduction

Automated fixture analysis and planning are essential for unmanned manufacturing, particularly in small-batch machining and assembly. However, fixturing and fixture planning are among the least solved challenges facing unmanned, flexible manufacturing systems today. Thus it is common to see manufacturing systems in which CNC machine tools automatically cut parts and coordinate-measuring machines inspect them, but in which people are still required to locate parts on pallets and clamp them in place. The specification of fixtures for producing a part is likewise dependent on people, requiring the skills of a machinist or manufacturing engineer. As an alternative, we are exploring automated fixture analysis and planning as a component of a computational system for concurrent product and process design. The fixture analysis is performed by a module called the fixture agent which interacts with other modules, including a geometric solid modeler and a machining sequence planner, so that fixturing and machining plans are developed concurrently as the design progresses (Cutkosky and Tenenbaum, 1990).

An important part of the philosophy of concurrent design is that fast, approximate analyses are used to give immediate feedback to the designer during early design stages, while more detailed analyses are used during final design and process planning, when more information about expected cutting forces, tolerances, etc., is available. As a consequence, it is necessary for modules like the fixture agent to be able to reason at multiple levels of detail, so that simple questions such as "Can this part be held in a vise?" are answered with a minimum of computation, leaving numerical analyses for more difficult questions such as "Will the part deform too much if I remove this rib?"

At present, the fixture agent has little "deep" knowledge of fixturing and instead relies on rules and simple geometric and kinematic checks for choosing fixtures, based on the dimensions of the workpiece and the expected cutting operations. As such, it is limited to a small repertoire of machining operations. The work described in this paper is part of an ongoing effort to model the process of work-holding more accurately and to provide the fixture agent with a powerful set of tools for fixture planning and analysis, including rules, numerical procedures and symbolic "reasoning from first principles."

The work in this paper draws upon previous geometric and kinematic analyses of robotic grasp and motion planning (e.g., Mason and Salisbury, 1985; Lozano-Perez, 1983) and fixture analysis (Asada and By, 1985; Ohwovoriole and Roth, 1981; Chou, Chandru, and Barash, 1989; Mani and Wilson, 1988; Bausch and Youcef-Toumi, 1990). However, the focus of this paper is the analysis of fixturing with friction, a relatively unexplored subject. Indeed, at the time the approach in this paper was developed, we found no comparable analysis. Recently, however, an analysis by Sakurai (1990) has appeared in which friction is considered for parts held by strap clamps. Although Sakurai uses a different approach, involving optimization, to solve for the friction limits, the results he obtains are equivalent to those that the analysis in Section 4.3 obtains for a part held by strap clamps.

The importance of modeling friction becomes clear when we recognize that common fixturing arrangements, such as a part clamped in a vise or held down with strap clamps, rely on friction for holding the part. In such cases, an obvious question is "How hard should one clamp?" Clamping harder than necessary may damage the part or produce deformations that reduce the final part accuracy. On the other hand, clamping too gently may permit the part to slip during machining, and be ruined.

Machinists learn to estimate clamping forces based on a variety of factors including the workpiece material (e.g., aluminum versus plastic), geometry (e.g., whether the part has thin walls or other easily deformed sections), the required tolerances and the expected cutting forces. The process of setting clamping forces is not entirely "open-loop" since the machinist feels the resistance in the crank of a vise and may tug on a clamped part to check that it is secure. Even so, the estimation of clamping forces is difficult and errors may occur, perhaps due to unexpected variations in cutting forces or the coefficient of friction. For unmanned manufacturing, we need a way of replacing the machinist's skill in assessing clamping forces and arrangements. Like the machinist, we need to consider geometric, kinematic, and force constraints in our fixture planner.

Contributed by the Production Engineering Division for publication in the JOURNAL OF ENGINEERING FOR INDUSTRY. Manuscript received July 1989; revised August 1990.

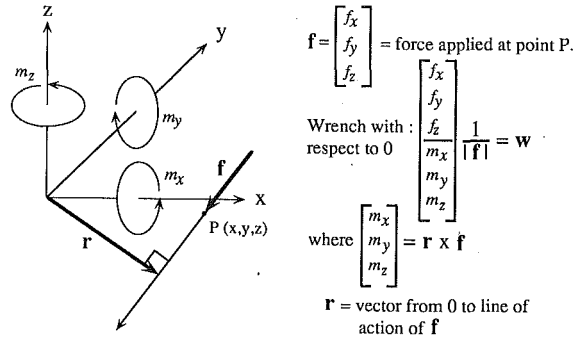

Fig. 1 A system of forces can be combined into a force along a unique line and a couple in a plane perpendicular to this line. This equivalent force and couple combination is called a wrench.

In the following sections some of the issues involved in fixture planning are first reviewed. An approach to fixture analysis is then presented, concentrating on kinematic issues and the modeling of friction to predict whether a part will slip for a given set of forces. Limit surfaces are constructed in force/moment space as a convenient formalism for reasoning about friction and for determining when and how clamped parts may slip. When used in the absence of deformation information, approximate limit surfaces are constructed, which permit estimates of the friction limits to be made. With more detailed information (e.g., pressure distributions supplied by an FEM analysis of the clamped part), precise limit surfaces can be constructed.

2 Issues in Fixture Planning

Fixture planning involves analyses at several different levels. In approximate order of increasing computational effort (and decreasing frequency of use) these are: geometric, kinematic, force, and deformation analysis.

Geometric Analysis. Geometric analysis in fixture planning has much in common with geometric analysis for robot grasp planning and motion planning (Lozano-Perez, 1983) and a variety of other subjects that involve spatial reasoning. Foremost, it is necessary that the proposed fixturing arrangement not interfere with the expected tool path, that the fixtures do not restrict access to features being machined, and that the fixturing elements themselves can access desired faces or other features for clamping. For the fixture agent, rules are first applied to determine whether the workpiece is suitable for holding in a vise or strap clamps, etc. Next, interference and access checks are performed, using approximate bounding volume representations of the features, clamping elements, and swept tool paths for speed. The remaining "clampable areas" on the workpiece faces are analogous to "free space" in robot motion planning and are represented using the approximate cell decomposition method (Lozano-Perez, 1983). After the geometric constraints are satisfied, heuristic objective functions are applied to reduce the number of candidate clamping arrangements. These heuristic functions essentially try to maximize the clamping stability, but do not apply the more formal analyses discussed in Sections 3 and 4.

Kinematic Analysis. Kinematic analysis of fixturing includes determining whether a fixture arrangement will correctly locate a part and whether it constrains the part with respect to cutting forces. For correct location, the fixturing elements should completely specify the position and orientation of the part with respect to desired datum surfaces, but should not overdetermine the location. For complete constraint, we require that contact forces applied by the fixturing elements (with or without friction) completely span the vector space of possible cutting forces. The approach to kinematic analysis pursued in the fixture agent is described briefly in Section 3.

Force Analysis. Force analysis is concerned with checking that the forces applied by the fixtures are sufficient to maintain static equilibrium in the presence of cutting forces. For fixturing arrangements that rely on friction, this entails a friction analysis as discussed in Section 4. We note that in contrast to the geometric and kinematic analyses, which can be applied when only the shape of the part is known, this analysis is useful only in the context of a machining plan with expected cutting forces.

Deformation Analysis. Deformation analysis is the final and most computationally intensive step. The concern is that a part may deform elastically and/or plastically under the influence of cutting and clamping forces so that the desired tolerances will not be achieved. Deformation is particularly a concern with flexible parts and with parts in which a great deal of material is removed. The application of finite element analysis is described by Sakurai (1990) and Lee and Haynes (1987). An FEM analysis also permits an accurate assessment of pressure distributions on the clamping surfaces and, consequently, a more precise version of the friction analysis. We are starting to pursue finite-element methods to predict workpiece deformation in the fixture agent. However, this work will not be described in this paper.

3 Kinematic Analysis of Fixtures

Kinematic analysis of fixturing has been addressed by a number of investigators including Asada and By (1985), Ohwovoriole and Roth (1981), Chou, Chandru, and Barash (1989), Mani and Wilson (1988), and Bausch and Youcef-Toumi (1990). In particular, Chou, Chandru, and Barash (1989) provide a careful analysis of form-closure and force equilibrium constraints for fixture analysis, drawing upon earlier work introducing screw theory for the analysis of robotic grasping and component assembly. The approach used by our fixture agent is similar, except that we include the extra contact forces due to friction.

In this section we summarize the kinematic analysis used in the fixture agent, focusing on those aspects that establish the framework for the force and friction analysis described in Section 4. We refer the reader to Mason and Salisbury (1985), Ohwovoriole and Roth (1981), Chou, Chandru, and Barash (1989) for a more detailed explanation of the underlying twist/wrench formalism. For the purposes of this section, it suffices to know that if a force, $\mathbf{f} = [f_x, f_y, f_z]^T$, is applied at a point, P, on a workpiece, the resulting 6-element wrench with respect to the origin is $w = [\mathbf{f}^T, (\mathbf{r} \times \mathbf{f})^T]/|\mathbf{f}|$, as shown in Fig. 1. The velocity or motion complement to a wrench is a twist. For a 6-element vector of rotational and translational motion at the origin, $\mathbf{v} = [\omega_x, \omega_y, \omega_z, v_x, v_y, v_z]^T$, the resulting twist at point P is $t = [\omega^T, (\mathbf{v} + \omega \times \mathbf{r})^T]$ where $\omega = [\omega_x, \omega_y, \omega_z]^T$.

The kinematic analysis begins by dividing fixturing elements into two classes: *passive* and *active*. The passive elements provide stationary locating surfaces and include parallel bars, the fixed jaw of a vise, V-blocks, and so forth. The active elements are movable and are used for applying forces. Active elements include hydraulic plungers, toggle clamps, strap clamps, and the movable jaw of a vise. A fixturing arrangement of passive and active elements should satisfy the principles of *complete location* and *kinematic constraint* (Asada and By, 1985).

Complete Location. Ignoring friction, the intersection of contact twists over all passive or locating elements should be a null set:

$$t_1 \cap t_2 \cap \ldots \cap t_n = \emptyset \qquad (1)$$

For example, the block held in the vise of Fig. 2(*a*) is not located in the (x, z) plane and has three degrees of freedom.

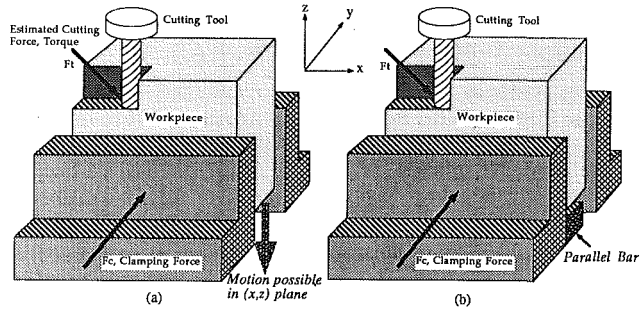

Fig. 2 In Fig. 2(*a*), the block is constrained by friction but is not located in the (*x*, *z*) plane and does not have "complete location." In Fig. 2(*b*), the block is unlocated only along the *x* axis.

Adding a parallel bar, as in Fig. 2(*b*), reduces the number of degrees of freedom to one. In practice, such clamping arrangements are often acceptable. For example, a machinist may use the fixturing arrangement in Fig. 2(*b*), locating the block in the *x* direction with a touch probe.

A corollary to the complete location principle is that the location of a part should not be overdetermined. In other words, if any of the passive fixturing elements is removed, the intersection of the contact twists should no longer be a null set. To illustrate this principle, we consider the contact twists for the fixed and movable jaws of the vise in Fig. 2(*a*) or (*b*) and observe that they are redundant:

$$\text{Twists from face "A" } \mathbf{T}_{n_A} = \begin{bmatrix} 0 & 0 & 0 \\ 1 & 0 & 0 \\ 0 & 0 & 0 \\ 0 & 1 & 0 \\ 0 & 0 & 0 \\ 0 & 0 & 1 \end{bmatrix}$$

$$\text{Twists from face "B" } \mathbf{T}_{n_B} = \begin{bmatrix} 0 & 0 & 0 \\ -1 & 0 & 0 \\ 0 & 0 & 0 \\ 0 & -1 & 0 \\ 0 & 0 & 0 \\ 0 & 0 & -1 \end{bmatrix}$$

In other words, the parallelism of the block with respect to the (*x*, *z*) plane can be established using either the front "A" or back "B" faces of the block. Unfortunately, this ambiguity can result in a part that does not meet intended geometric tolerances. For example, suppose that the "A" face is not quite parallel with respect to the "B" face, which is a datum surface. The block should therefore be located with planar contact between the "B" face and the fixed jaw of the vise. However, if the vise has two rigid, parallel faces the block may adopt a number of orientations as shown schematically in the exaggerated views of cases (*a*) and (*b*) in Fig. 3. A better approach is to use a vise with a ball-joint on the movable jaw as in case (*c*) (like the pivoted foot of a hobbyist's C-clamp), that will adopt the orientation of face "A" and press face "B" firmly against the fixed jaw. The resulting arrangement also provides more reliable clamping, and a more accurate assessment of the friction limits, since the contact forces are better known. Similar principles have been proposed for modular fixtures by Mani and Wilson (1988).

Kinematic Constraint. Assuming that the clamping elements keep the part pressed against the locating elements, the union of contact wrenches over all locating elements should have rank 6:

$$w_1 \cup w_2 \cup \ldots \cup w_n = R^6 \qquad (2)$$

For robotic grasping, this condition has been called "force-closure." As Fig. 4 shows, a part clamped in a vise satisfies

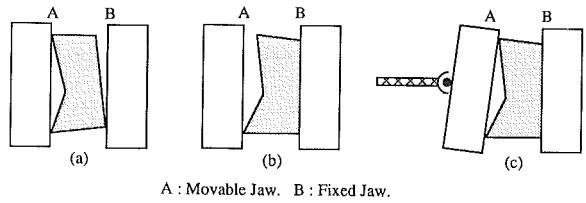

Fig. 3 Possible errors in clamping a block in a vise with two parallel faces (*a-b*) and solution involving one fixed and one pivoting face (*c*)

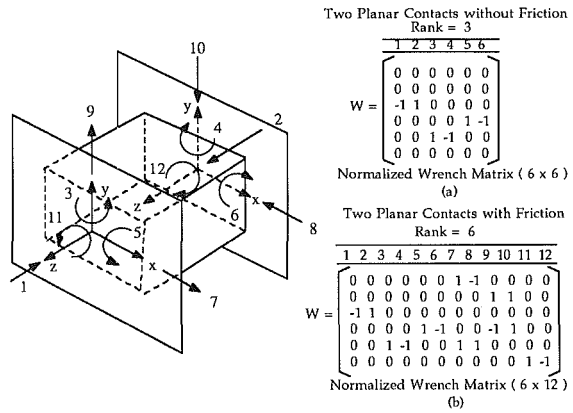

Fig. 4 Contact wrenches for a part clamped in a vise with and without friction

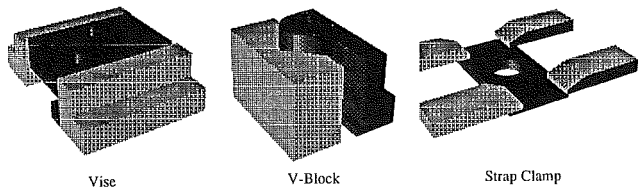

Fig. 5 Examples of arrangements in the fixture library that require friction

force-closure only if we consider the additional contact wrenches due to friction between the vise jaws and the part. A more conservative requirement would be to insist that a fixturing arrangement satisfy force closure even in the absence of friction. Where force-closure can be achieved without friction it is preferable. However, many commonly used fixturing arrangements, including the three pictured in Fig. 5 from the fixture agent's library, rely on friction. For such arrangements it is necessary to proceed to a force analysis with friction as described in the following section.

4 Force Analysis With Friction

The force analysis begins by applying the equations of static equilibrium. However, since fixturing arrangements are generally statically indeterminate, the equilibrium equations constrain the contact and friction forces, but do not uniquely determine them. The next step is to consider ways to determine when and how a clamped part may start to slip under the action of cutting forces and vibrations. This information is used to determine when to increase clamping forces and/or modify the fixturing arrangement. For this analysis, we build upon recent work in robotics including grasp planning and the pushing of objects in a plane, under the influence of Coulomb friction.

4.1 Friction Limit Surfaces. Since the fixturing arrangement is statically indeterminate we cannot determine all the contact forces or pressure distributions without an elastic analysis. We therefore seek a force analysis that does not require knowledge of the pressure distributions over all contact surfaces, but which provides insight as to how and when a part might slip.

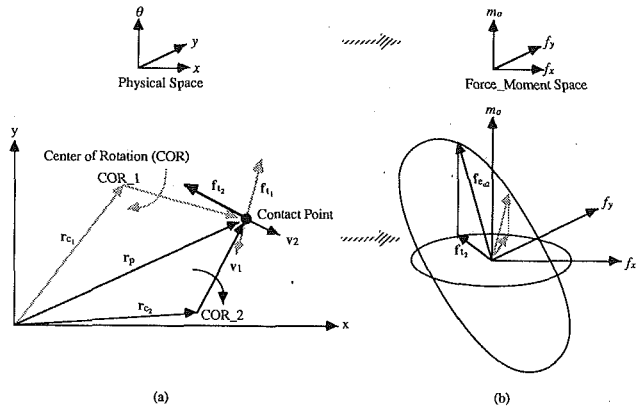

Fig. 6 The limit surface of a single point contact becomes an ellipse

This knowledge is useful for specifying clamping forces and/or adding extra fixturing elements to resist motion in the most vulnerable directions. In this analysis we assume that we can measure the forces applied by the active elements and adjust them at will.

The slipping analysis builds on recent work by Mason (1986), Peshkin (1986), and Goyal (1989) on the sliding of objects pushed in a plane with friction and on robotic grasps with friction (Cutkosky, 1989). The central idea is that once a part starts to slip, the instantaneous velocity and the resulting frictional force are uniquely related. By establishing a mapping between velocities and corresponding forces and moments, one can solve the inverse problem of determining how a part will slip in response to *applied* forces. The process of mapping between motions and forces results in a limit surface in force/moment space.

4.2 The Limit Surface for a Single Contact Point. As a starting point, consider a single point of contact against a face of a workpiece. The contact point is located by a vector, $\mathbf{r}_p$, with respect to the origin as shown in Fig. 6(*a*). Until the part slips, the friction force is undefined, but as soon as its starts to move with a velocity $\mathbf{v} = [v_x, v_y]^T$, [corresponding to motion about an instantaneous center of rotation (COR) located at a point $\mathbf{r}_c$] the magnitude and direction of the friction force are known:

$$\mathbf{f}_t = [f_{t_x}, f_{t_y}]^T = \mu f_n \frac{-\mathbf{v}}{|\mathbf{v}|} \tag{3}$$

where $\mathbf{v} = \omega \times (\mathbf{r}_p - \mathbf{r}_c)$, $(\mathbf{r}_p - \mathbf{r}_c)$ is a vector from the COR to the contact and ω is the angular velocity with respect to the COR.

Next, the contact friction force, $\mathbf{f}_t$, is transformed to a resultant three-element force/torque vector at the origin: $\mathbf{f}_o = [f_{t_x}, f_{t_y}, m_o]^T$ (where $m_o = \mathbf{r}_p \times \mathbf{f}_t$). If one constructs the vector $\mathbf{f}_t$ for every possible location of $\mathbf{r}_c$ and plots the results in (f_{t_x}, f_{t_y}, m_o) space, a limit surface in force/moment space is obtained. As Fig. 6(*b*) shows, the limit surface forms a circle in the (f_x, f_y) plane corresponding to the constant magnitude of $\mathbf{f}_t$. In the three-dimensional (f_{t_x}, f_{t_y}, m_o) space the curve becomes an ellipse. The moment is largest when the center of rotation is on a line containing $\mathbf{r}_p$ and there is a singularity ($|f_t|$ is undefined) when the COR is directly beneath the contact point (i.e., $\mathbf{r}_p = \mathbf{r}_c$).

Figure 6 also indicates how to use the limit surface to solve the inverse problem of predicting the slipping motion for an applied force. First, note that if the magnitude of a force, $\mathbf{f}_e$, applied to the contact is smaller than $|f_t|$, the part will not slip. If we take the resultant force and moment vector, $\mathbf{f}_{e_o} = [f_{e_x}, f_{e_y}, m_o]^T$, at the origin and plot it in force and moment space we see that $\mathbf{f}_{e_o}$ lies in the plane of the ellipse. As $|f_e| \rightarrow |f_t|$, $\mathbf{f}_{e_o}$ will intersect the limit surface as the contact starts to slide in the direction of $\mathbf{f}_e$. Finally, if $|f_e| > |f_t|$, quasistatic equilibrium will not be satisfied and the contact will not only slip but will accelerate.

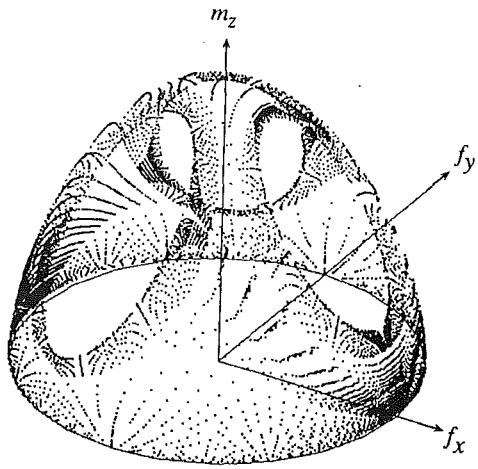

Fig. 7 Friction limit surface of three supporting points, obtained by scanning the COR over the (*x*, *y*) plane

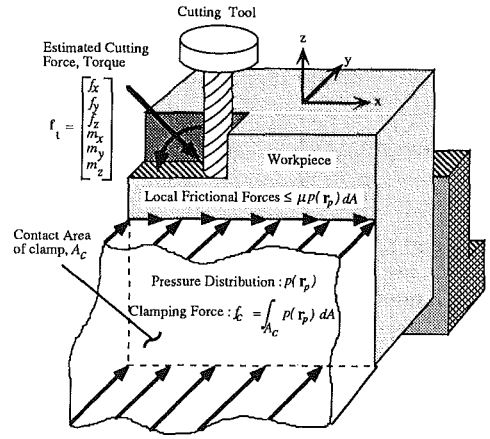

Fig. 8 A rectangular block is held in a vise. The details of the pressure distribution are not known and depend on the location of the cutting tool and the cutting conditions.

4.3 Limit Surfaces for Multiple Points of Contact. The results for a single point of contact are easily extended to multiple contacts. For two or more contact points, the limit surface encloses a volume of "safe" forces and moments that can be applied without slipping. Goyal (1989) shows that the limit surface for a combination of contact points can be constructed as the Minkowski sum of the ellipses for each contact. He also shows that the unit normal where an applied force/moment vector, $\mathbf{f}_{e_o}$, intersects the surface, gives the direction of slipping motion.

The limit surface can also be constructed for multiple contacts simply by scanning the COR over all points in the plane and plotting the resultant force and moment vectors. For example, the limit surface for a tripod of contact points, obtained by scanning the COR over the (*x*, *y*) plane, is shown in Fig. 7. In this case, the limit surface encloses an approximately ellipsoidal volume with three facets. The facets correspond to singularities where the COR is directly under one of the three contact points. For larger numbers of contact points the facets shrink in size, and for continuous pressure distributions they vanish.

In investigating the motion of an object pushed in a plane, Mason (1986) points out that a tripod of contact points is particularly useful since any pressure distribution that satisfies the equilibrium equations for stability with respect to the plane can be approximated by a tripod with the same centroid:

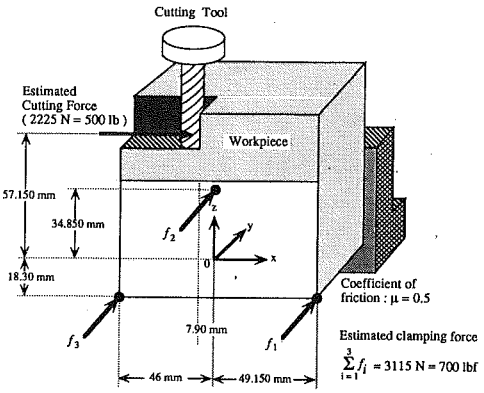

Fig. 9 A rectangular block is held in a vise with a pressure distribution that is approximated by a tripod of forces that satisfies the same equilibrium.

$$[X]\cdot\mathbf{f}=f_n\begin{bmatrix}x_o\\ y_o\\ 1\end{bmatrix} \tag{4}$$

where $\mathbf{f}$ is a vector of the supporting forces, $[x_o, y_o]^T$ is the centroid location, $[X] = \begin{bmatrix}x_1 & x_2 & x_3\\ y_1 & y_2 & y_3\\ 1 & 1 & 1\end{bmatrix}$ gives the locations of the contacts and f_n is the normal force. If the locations of the contact points are fixed, then the magnitudes of the normal forces at each point are uniquely determined by equation (4). The idea is to find a tripod that produces a limit surface nearly identical to the limit surface of the actual pressure distribution. But since the actual pressure distribution is unknown, there are many feasible approximating tripods, corresponding to different locations of the contact points within the contact area. Mason (1986) and Peshkin (1986) therefore define loci of centers of rotation corresponding to the set of all possible tripods that satisfy equation (4) and lie within the contact area. The result is that while the exact motion of the sliding object cannot be predicted for an applied force and moment, bounds on the motion can be established.

5 Applying Limit Surfaces to Fixturing

We now consider a simple example to explore how limit surfaces can be used for analyzing fixtures with friction. Figure 8 shows a rectangular block held in a vise which, in keeping with the kinematic principles of Section 3, has a ball joint on the movable jaw.

The part was located using a parallel bar, but the bar has been removed during machining to avoid possible interference with the tool. The cutting forces are expressed by a 6-element force/moment vector, $[\mathbf{f}_e^T, \mathbf{m}_e^T]$, which produces a resultant vector, $[\mathbf{f}_{e_o}^T, \mathbf{m}_{e_o}^T] = [J]^T[\mathbf{f}_e^T, \mathbf{m}_e^T]$ at the origin, where $[J]$ is a 6×6 cartesian transformation matrix. The clamping force, $\mathbf{f}_c = [0, f_c, 0]^T$, produces an (unknown) pressure distribution over the two vise jaws. For equilibrium,

$$f_c=\int_A p(\mathbf{r}_p)dA \tag{5}$$

$$\mathbf{m}_{f_o}=\int_A \mathbf{r}_p\times\mu\frac{\mathbf{v}}{|\mathbf{v}|}p(\mathbf{r}_p)dA \tag{6}$$

where $\mathbf{m}_{f_o}$ is a frictional moment with respect to the origin and $\mathbf{r}_p = [x, y, z]^T$ is a vector from the origin on a contact face to an element of the contact area. We will assume that we also know $\mathbf{f}_c$, perhaps because the vise is instrumented with strain gages. Also, since one of the vise jaws is pivoted, the center of pressure is at the center of the face (in line with the ball joint.)

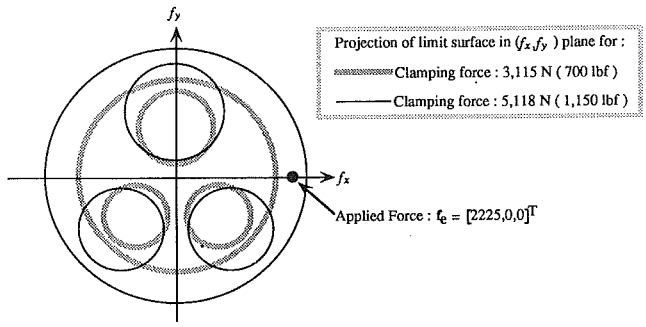

Fig. 10 Projection of the vise limit surface in the (f_x, f_y) plane. If the clamping force is increased to 5,118N (1,150lbf), the cutting force no longer produces slipping.

We want to clamp hard enough to prevent slipping, but not excessively hard. Now suppose that the pressure on the front face is primarily confined to three contact areas (perhaps due to a lack of flatness in the part) as indicated in Fig. 9. In this case we could immediately construct a limit surface as in Fig. 7.

However, it is too time consuming to construct such surfaces numerically for on-line fixture planning. For example, it took 5 CPU minutes on a 68020-based workstation to compute the limit surface in Fig. 7 by scanning the COR location over the plane and approximately 2 CPU minutes to achieve a comparable resolution by the Minkowski sum method. The computational time for the COR scanning method increases as the product of the number of contact points and the number of COR locations. The computation time for the Minkowski sum method grows more rapidly. For n points of contact and a resolution of m points on the ellipse (see Fig. 6) associated with each point, the computations grow as $(m + 1)^n$.

In practice, considerable savings can often be achieved. For example, when using the scanning method, a nonuniform spacing in which COR locations are scanned slowly in the vicinity of supporting points and more rapidly elsewhere gives good results. In addition, for approximately symmetric pressure distributions, the COR need only be scanned along a few lines that pass through the origin, to obtain some representative projections on planar cross-sections. Similarly, for the Minkowski sum method, only the projections on a few subspaces are typically necessary. Nonetheless, it takes 15 CPU minutes on the same workstation to compute a limit surface comparable to that shown in Fig. 7 for eight supporting points. Thus, there is a motivation to find a fast, approximate method for determining the limit surface for arbitrary pressure distributions.

Such an approach is to fit an approximating ellipsoid to the data. Since the ellipsoid has an analytic form, we can rapidly determine whether the expected cutting forces and moments will be contained within it. In constructing the ellipsoid we first recall that the limit surface for any pressure distribution forms a circle on the (f_x, f_y) plane. In addition, we know that the maximum moment will occur for the case where the COR is at the origin (which, in this case, is also the center of pressure). Using these constraints, an approximating ellipsoid is found as follows:

(*1*) Find the point of maximum moment, $\mathbf{p}_{\max} = (f_x, f_y, m_{o_{max}})$, (where the COR is at the origin) and plot it in (f_x, f_y, m_o) space. This defines the end points, the tilted angles with respect to the f_x axis and f_y axis and major axis of the ellipsoid.

Let $c = \sqrt{f_x^2+f_y^2+m_o^2}$.

(*2*) Find the (3×3) orthonormal transformation matrix, $\mathbf{R}$, between the original (f_x, f_y, m_o) coordinate system and a new (f_x', f_y', m_o') frame aligned with the major axis of the ellipsoid.

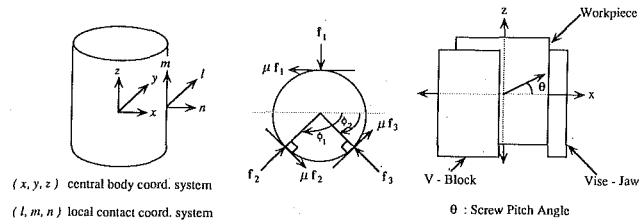

Fig. 11 A cylinder is held between a V-block and a plate with 3 line contacts.

(3) Find the points p_1, p_2 where the circle in the (f_x, f_y) plane intersects the f_x and f_y axes and express them in the (f_x', f_y', m_o') frame.

(4) Solve for the ellipsoid that contains $m_{o_{max}}$ as its end point and includes the points p_1', p_2':

$$\left(\frac{p_{1x}'}{a}\right)^2+\left(\frac{p_{1y}'}{b}\right)^2+\left(\frac{p_{1z}'}{c}\right)^2=1 \tag{7}$$

$$\left(\frac{p_{2x}'}{a}\right)^2+\left(\frac{p_{2y}'}{b}\right)^2+\left(\frac{p_{2z}'}{c}\right)^2=1 \tag{8}$$

where c is given by step 1.

For continuous pressure distributions, or pressure distributions with many contacts, the facets on the limit surface can be ignored. But for pressure distributions with just a few, concentrated pressure regions (e.g., clamping a thin piece of metal with two or three strap clamps), the volumes corresponding to the facets should be removed. We can do this by constructing planes corresponding to the facets:

$$\left(\left(\frac{x}{a}\right)^2+\left(\frac{y}{b}\right)^2+\left(\frac{z}{c}\right)^2-1\right)\prod_{i=1}^{2n}(\mathbf{p}_i\cdot\mathbf{n}_i-\mathbf{d}_i)<0 \tag{9}$$

where $\mathbf{p}_i$, $\mathbf{n}_i$ and $\mathbf{d}_i$ represent a point on the facet, a normal vector on the facet and a distance from the origin to the facet, respectively.

Returning to the example, we assume that the cutting force is entirely in the (x, z) plane where $\mathbf{m}_e = [0, 0, 0]^T$ and $\mathbf{f}_e = [2225, 0, 0]^T$. The coefficient of friction is assumed to be 0.5. The magnitudes of the contact forces, $\mathbf{f} = [f_1, f_2, f_3]^T$ (see Fig. 9), are determined from equation (4):

$$\begin{bmatrix} 49.15 & 0 & -46 \\ -18.30 & 34.85 & -18.30 \\ 1 & 1 & 1 \end{bmatrix}\cdot\mathbf{f}=\begin{bmatrix} 0 \\ 0 \\ 3{,}115 \end{bmatrix}. \tag{10}$$

As shown in Fig. 10, the resultant force vector, $[\mathbf{f}_{e_o}^T, \mathbf{m}_{e_o}^T]$, is outside the limit surface and the part will slip. However, if we increase the clamping force to 5,118N (1,150lbf), the limit surface expands and the cutting force will no longer produce slipping.

6 Extensions to Three-Dimensional Problems

Although some fixturing problems are essentially planar (e.g., a block held in a vise or a plate held down with strap clamps), others require a three-dimensional treatment. To address such problems we extend the planar sliding analysis to include rigid bodies with up to five degrees of freedom[1]. As in the planar case, the limit surface represents a mapping between possible motions of the sliding body and corresponding forces and moments taken with respect to some reference frame. Also as in the planar case, the limit surface can be numerically generated by scanning over the space of all possible directions of motion and plotting the corresponding force/torque vectors. However, we now have six-element force/torque vectors that must be plotted in a six-dimensional force/torque space. While

[1]A part can have up to five degrees of freedom in sliding without breaking contact.

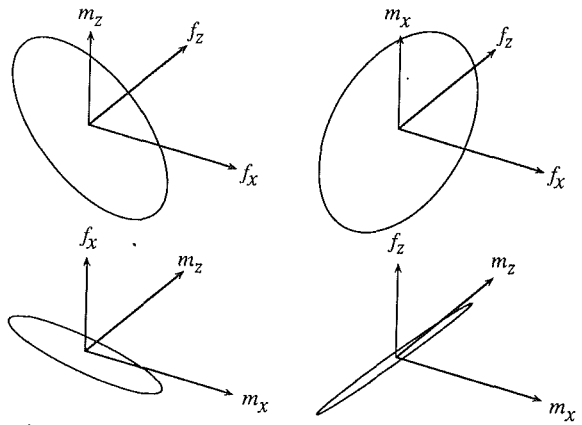

Fig. 12 Projections of the limit surface for the first line contact, expressed in the workpiece coordinate frame

the resulting limit surfaces lack the intuitive appeal of the surfaces for planar problems, three-dimensional projections of the limit surfaces can be plotted on subspaces for visualization.

A potential drawback is that scanning over the space of all possible motions could be very time consuming. Fortunately, most fixture arrangements only have two or three degrees of freedom for sliding. This is basically a result of the need to locate and constrain the workpiece. A fixture arrangement with more than three degrees of freedom for possible sliding motions is unlikely to satisfy the force-closure requirements of Section 3 and would not locate the part adequately. Therefore, it is useful to apply the kinematic constraints of Section 3 before scanning over the space of possible sliding motions. The kinematic constraints produce a limit surface with non-zero projections on only a few subspaces.

An approach to treating three-dimensional problems is as follows:

(1) Determine the contact type and the sliding degrees of freedom (i.e., the instantaneous motions for which the contact types remain unchanged) by taking the intersection of contact twists, as in Section 3.

(2) Find the limit surface, expressed in the contact coordinate frame, for each contact subject to the kinematic constraints from Step 1. These limit surfaces will typically be quite simple; perhaps just a circle or an ellipse in the tangent plane of the contact.

(3) Transform the limit surface of each contact to a limit surface expressed in the central coordinate system of the workpiece. As the limit surfaces are transformed to the workpiece coordinates, they typically become more complex as extra torques are picked up due to the contact forces acting at some distance from the central axes. However, only projections of the limit surface on those subspaces in which motion is possible need be considered.

(4) Take the Minkowski sum of the limit surfaces from Step 3 to obtain the surface for the entire arrangement. Again, it is only necessary to consider projections on the subspaces for which motion is possible.

(5) Test expected cutting forces and torques, expressed in the workpiece coordinate system, against the limit surface to determine whether the part will slip, and if so, in what direction it will move.

The approach can be illustrated by the case of a cylinder held between a flat plate and a V-block. Although this is a simple example, and the final result is perhaps obvious from symmetry, it is three-dimensional and will be solved as a general three-dimensional problem.

6.1 Example: Solving for the Limit Surface of a Cylinder in a V-Block as a 3D Problem. Figure 11 shows a cylindrical workpiece clamped between a flat plate and a V-block. The

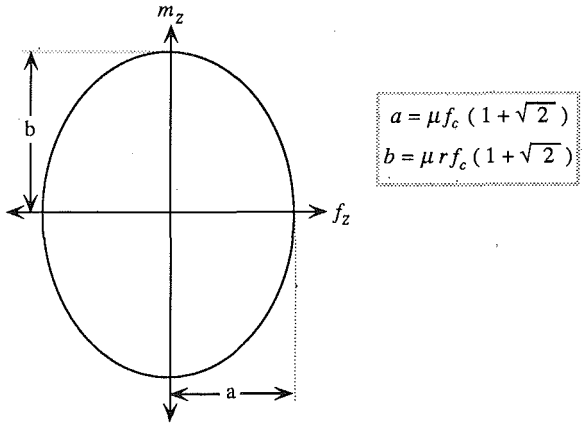

Fig. 13 The final limit surface for a cylinder held in a V-block becomes an ellipse.

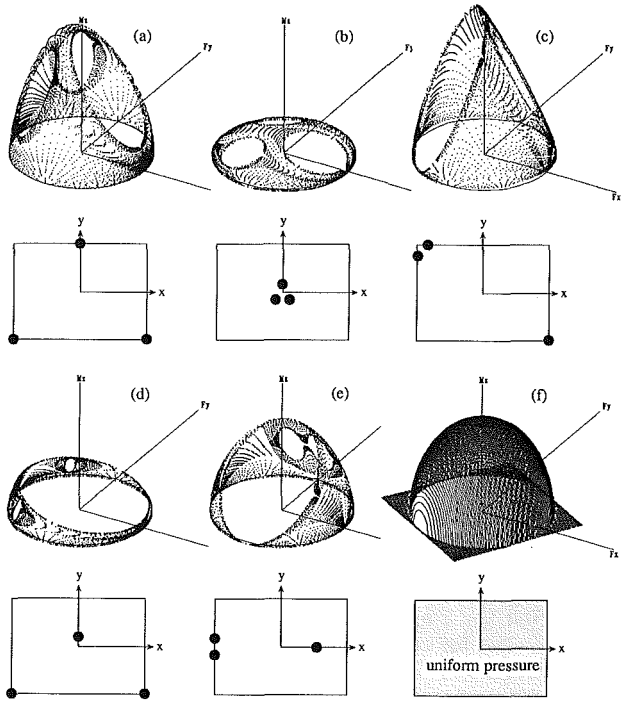

Fig. 14 Different friction limit surfaces produced by different contact assumptions that satisfy the same equilibrium equations.

arrangement results in three line contacts and kinematically constrains the cylinder so that the only possible sliding motions are translations along the z axis and rotations about the z axis. In fact, all motions of the cylinder can be represented by a screw axis along the centerline of the cylinder and a finite pitch angle, θ, corresponding to a ratio of translation to rotation as shown in Fig. 11. Therefore, we expect that the limit surface for this arrangement will have a non-zero projection only on the (f_z, m_z) plane. The first step is to apply the kinematic constraints to determine the vector space of possible motions, expressed in the local (l, m, n) coordinate system of each contact. The n axes are normal to the surface of the cylinder and the m axes are aligned with the centerline of the cylinder, as in Fig. 11. In this example, only translations along the l and m axes are possible for each line contact. The limit surface for each contact is therefore simply a circle in the (f_l, f_m) plane. (If the contact friction were anisotropic, perhaps due to fine grooves on the surface of the cylinder, the local limit surfaces could be expressed as ellipses.)

Transforming the local, circular limit surfaces to the (x, y, z) coordinate system of the cylinder results in more complicated surfaces, with torque components. The simplest of these is for

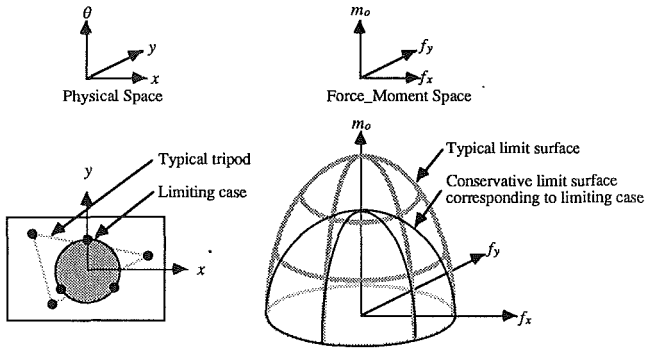

Fig. 15 A conservative lower bound on the limit surface for all pressure distributions known to lie primarily outside a central region

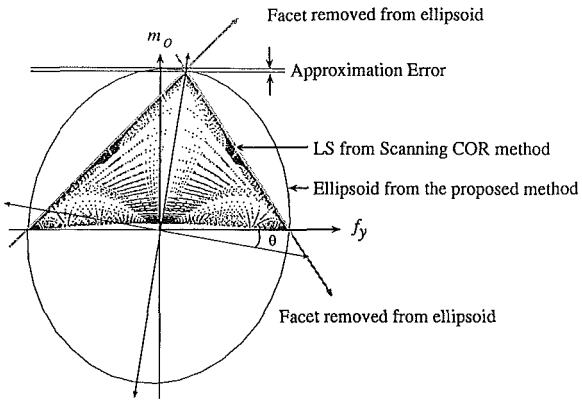

Fig. 16 The ellipsoid has an approximation error depending on the angle of inclination, $\theta = \tan^{-1} \frac{f_{l_{vertex}}}{m_{o_{max}}}$ (shown for the case of two strap clamps).

the first contact, for which the l and n axes happen to be aligned with the x and y axes, respectively, so that a four-dimensional limit surface (f_x, f_z, m_x, m_z) results. The projections of the resulting limit surface on four three-dimensional subspaces, (f_x, f_z, m_z), (f_x, f_z, m_x), (f_x, m_x, m_z) and (f_z, m_x, m_z), are shown in Fig. 12. Not surprisingly, they are ellipses since the moments all vary as $r \times f$. The final step is to sum the limit surfaces, expressed with respect to the (x, y, z) coordinate system, for the three line contacts. Only the projections on the f_z and m_z plane need be considered since motions are possible only along and about the z axis. All other sliding forces and moments will cancel. As expected, the final result is an ellipse, as shown in Fig. 13. The length of the major axis of the ellipse for a 90deg V-block ($\phi_1 = 135$deg and $\phi_2 = 45$deg), for example, is $b = \mu r f_c(1 + \sqrt{2})$ and the minor axis is $a = \mu f_c(1 + \sqrt{2})$ where r is the radius of the cylinder and f_c is the clamping force.

7 Discussion

Once constructed, the limit surface for a two- or three-dimensional fixture arrangement can be compared against all anticipated forces to test for slipping. However, a number of practical issues remain to be solved before the method can be used in on-line fixture planning. The most important of these is that neither the pressure distributions nor the cutting forces are exactly known. Therefore, we seek a conservative lower-bound on the limit surface that will apply to all feasible pressure distributions, and against which we can test expected cutting forces with some factor of safety. As it happens, many different pressure distributions have similar limit surfaces. For example, Fig. 14 shows the limit surfaces for several tripods and for a uniform pressure distribution, all of which satisfy the same equilibrium conditions and have the same center of pressure as the tripod for the block held in a vise in the example of

Section 5. Therefore, they could all theoretically have been applied to the same example.

The intersection of all the limit surfaces in Fig. 14 with the (f_x, f_y) plane is a circle of radius $f_t = \mu\Sigma f_{n_i}$, where $\mu\Sigma f_{n_i} = 3{,}115N(700lbf.)$ [For case (f), $f_t = \mu\int_A p(\mathbf{r})dA$, where $\int_A p(\mathbf{r})dA = 3{,}115N$.] However, the ability of the different contact arrangements to resist moments in the plane depends strongly on the spacing between the points. When the points are close together, as in case (b), the limit surface is very low. We also see that an asymmetrical arrangement of the contact points results in a correspondingly skewed limit surface, whereas a symmetric arrangement gives a symmetric surface. In the extreme case where two of the contact points are nearly coincident as in case (c), the tripod limit surface approaches that of a dipod. We also note that the case of a uniform pressure distribution is more conservative than case (a) since the maximum frictional moment is proportional to the first polar moment of the pressure distribution.

More importantly, it is evident that a variety of contact positions produce similar limit surfaces. In fact, if we are able to rule out cases such as (b) and (d) in Fig. 14, we can construct a conservative limit surface that will handle all expected cases. For example, Fig. 15 shows a lower-bound on the limit surface for all cases where the contact points are known to lie outside some central region.

If a finite-element analysis is performed on the clamped part (e.g., following the approach in Lee and Haynes, 1987), then the exact pressure distribution over the clamping surface can be obtained and the exact limit surface computed. However, for concurrent design it may be desirable to obtain a rough estimate of the friction limits when a finite-element analysis is impractical, either for reasons of speed or because the design is still in an early stage. In this case it is necessary to determine, perhaps using knowledge about the flatness of the clamped part, what the *approximate* pressure distribution is. Failing this, one might establish a space of "reasonable" pressure distributions and then compute the innermost limit surface, corresponding to the worst-case pressure distribution in that space. We are currently pursuing both approaches.

A second practical issue involves the accuracy of the ellipsoidal approximation. In particular, as seen in Fig. 16, there is an error in the approximation when $m_{o_{max}}$ does not coincide with the end point of the ellipsoid. The relative magnitude of the error depends on the angle of inclination of the ellipsoid, which in turn depends on the degree of asymmetry in the contact arrangement. Thus, if we have prior knowledge that the contact pressure is highly asymmetric we may wish to use a different procedure to find the ellipsoid that includes the circle of radius $\Sigma\mu f_n$ in the (f_x, f_y) plane, and is tangent to the plane $z = m_{o_{max}}$ at the point $(f_x, f_y, m_{o_{max}})$.

8 Conclusions and Future Work

A limitation of process planners using empirically derived expert rules is that they have no "deep" knowledge of the underlying physics and geometry. As a result, it becomes difficult to make accurate plans where there are competing goals, such as the desire to specify aggressive speeds and feeds, the desire to prevent the part from slipping and the desire to prevent deformation of the workpiece due to clamping and cutting forces. We believe that a solution to such problems (and to related problems such as robot grasp planning and assembly motion planning) will require the ability to reason about geometry, kinematics, and mechanics. The analysis in this paper is part of an effort to provide such abilities for a fixture planning module.

The friction analysis involves the use of limit surfaces in force/moment space. These surfaces form a convenient tool for reasoning formally about friction. They are also convenient for planning, since any series of anticipated forces and moments can be tested against the limit surface. If the forces and moments fall inside the surface, the arrangement is "safe." While the limit surface approach is promising, a number of issues require further exploration before it can be used with arbitrary fixture arrangements. Foremost among these is the trade-off between accuracy and computational efficiency. An exact limit surface can only be computed if the pressure distribution is known, which in turn would require a complete elastic analysis of the part. But an exact limit surface is hardly necessary, or even worthwhile, when we consider that cutting forces and the coefficient of friction can only be approximately predicted for typical machining operations. The limit surfaces depend linearly on the coefficient of friction, which is notoriously hard to predict in the presence of cutting fluids, etc. Therefore, an additional area of work is the experimental verification of the predicted limits.

From a broader perspective, fixture planning is an example of the kind of problem where, for rapid response, it is important to establish the necessary level of abstraction and detail for answering questions. At the simplest level, questions about possible collisions with the cutting tool may be answered by checking for interferences among bounding boxes. At a more involved level, questions about the ability to locate a part may be answered by evaluating the rank space of contact twists. Similarly, questions about the required clamping forces can be answered by examining limit surfaces. Finally, if it is necessary to determine whether strains will be large enough in certain regions of the part to cause yielding, a finite element analysis may be needed.

9 Acknowledgment

The authors would like to thank Rob Howe and Prasad Akella for many helpful discussions and constant encouragement. This work was supported by the National Science Foundation under NFS Grant DMC-8618488 and DARPA under N00014-88K-0620. Part of the material in this paper was presented at the 1989 NSF Design Theory and Methodology Conference, Amherst, MA, June 1989.

References

1 Asada, H., and By, A. B., 1985, "Kinematic Analysis of Workpart Fixturing for Flexible Assembly With Automatically Reconfigurable Fixtures," *IEEE Journal of Robotics and Automation*, pp. 86–94, June.

2 Bausch, and J. J., and Youcef-Toumi, K., 1990, "Kinematic Methods for Automated Fixture Reconfiguration Planning," *Proceedings of 1990 IEEE International Conference on Robotics and Automation*, pp. 1396–1401, May.

3 Chou, Y-C., Chandru, V., and Barash, M. M., "A Mathematical Approach to Automatic Configuration of Machining Fixtures: Analysis and Synthesis," ASME Journal of Engineering for Industry, Vol. 111, pp. 299–306, November.

4 Cutkosky, M. R., and Tenenbaum, J. M., 1990, "A Methodology and Computational Framework for Concurrent Product and Process Design," *Mechanism and Machine Theory*, Vol. 25, No. 3, pp. 365–381, April.

5 Cutkosky, M. R., 1989, "Modeling and Sensing Finger/Object Contacts for Manipulation and Control," *Robotics Research—1989, Proceedings of the ASME Winter Annual Meeting*, pp. 181–188, San Francisco, CA, December 10–15.

6 Goyal, S. 1989, "Planar Sliding of a Rigid Body with Dry Friction: Limit Surfaces and Dynamics of Motion," PhD thesis, Cornell University, January.

7 Lee, J. D., and Haynes, L. S., 1987, "Finite-Element Analysis of Flexible Fixturing System," *Transactions of the ASME*, Vol. 109, pp. 134–139, May.

8 Lozano-Perez, T., 1983, "Spatial Planning: A Configuration Space Approach," *IEEE Transactions on Computers*, C-32, 2, February.

9 Mason, M. T., 1986, "Mechanics and Planning of Manipulator Pushing Operations," *The International Journal of Robotics Research*, Vol. 5, No. 3, pp. 53–71, Fall.

10 Mason, M. T., and Salisbury, J. K., 1985, *Robot Hands and the Mechanics of Manipulation*, The MIT Press, Cambridge, Mass.

11 Mani, M., and Wilson, W., 1988, "Automated Design of Workholding Fixtures Using Kinematic Constraint Synthesis," *Proceedings of the 16th North American Manufacturing Research Conference of SME*, Urbana-Champaign, May.

12 Ohwovoriole, M. S., and Roth, B., 1981, "An Extension of Screw Theory," ASME *Journal of Mechanical Design*, Vol. 103, pp. 725–735.

13 Peshkin, M. A., 1986, "Planning Robotic Manipulation Strategies for Sliding Objects," PhD thesis, Carnegie Mellon University.

14 Sakurai, H., 1990, "Automatic Setup Planning and Fixture Design for Machining," PhD thesis, Massachusetts Institute of Technology, February.